OPTIMAL DESIGN OF THE COMPENSATION NETWORKS OF AN INDUCTIVE WIRELESS POWER TRANSFER SYSTEM

PURPOSE. This paper presents an approach to the design of the compensation networks based on a genetic optimization algorithm. The algorithm is applied to compensation networks with T-topology, and considers the effects of the parasitic series resistances of their inductive components. The effectiveness of the algorithm is verified using Bode diagrams and simulation results.

DESIGN/METHODOLOGY/APPROACH. The paper at first describes the problem and the approach followed to reach a set of optimal solutions. Then explains the optimization algorithm, reports the obtained solutions, and selects the optimal Compensation Networks (CNs). Finally, the actual performance of the Wireless Power Transfer System (WPTS) when the selected CNs are used are checked.

FINDINGS. This approach gave interesting results and made available a number of different sizing solutions of complex networks in a very short time. Most of the obtained solutions outperform the widely-used Series-Series (SS) compensation; but an accurate post processing of the obtained result is mandatory in order to discriminate the solutions that could actually be implemented from those that in a real system would not give acceptable performance because of uncontrolled high frequency current oscillation.

ORIGINALITY/VALUE. This paper offers a rather new approach to solve the problem of sizing the compensation networks of a dynamic wireless power transfer system. This approach makes available a large number of candidate optimal solutions to the problem in a short time,

without requiring to solve complex system of equations.

1. INTRODUCTION

Inductive Wireless Power Transfer Systems (WPTSs) are based on the inductive coupling between two coils [1]. In addition to the main inductors, WPTSs are equipped with the Compensation Networks (CNs), which play a fundamental role in determining the overall system performance from the point of view of the power transfer and, in some applications, to enable additional functions [2]. CNs are formed by reactive elements whose value is determined by inverting the mathematical system of equations that relate the CNs reactances to the WPTS performance [3]. This operation is rather difficult when complex CNs topologies are considered, so that simplifying hypotheses are introduced to solve the equation system or numerical methods are applied to find a solution [4].

It is a rather common approach to solve problems related to engineering design using an optimization approach that considers two or more objective functions. This paper proposes to apply the genetic optimization approach [5,6] to the design of CNs having a T-topology, obtaining the values of the reactive elements that maximize the efficiency η and the transferred power P_L. This process does not invert the equation system above-mentioned and, in this way, complex CNs can be designed without the need of simplifying hypotheses and more reliable results can be obtained.

The paper is organized as follows. Section II describes the problem and the approach followed to reach a set of optimal solutions. Section III explains the optimization algorithm, reports the obtained solutions, and selects the optimal CNs. Section IV checks the actual performance of the WPTS when the selected CNs are used. Section V concludes the paper.

2. PROBLEM DESCRIPTION

The WPTSs are supplied by switching inverters that generate square or semi-square voltage waveforms at their outputs. The main circuit is equipped by two CNs, one of them, denoted as CN_t, is connected to the transmission stage, while the second, denoted as CN_r, is connected to the receiving stage. Usually the CNs work in resonant conditions and have a band pass behavior so that the current supplied by the inverter is nearly sinusoidal despite the actual waveform of its output voltage. For this reason, the problem of the CNs design has been faced considering the equivalent circuit of a generic WPTS, shown in Fig. 1, as supplied by a sinusoidal voltage $v_s(t)$.

The two CNs show the same T-topology reported in the left side of Fig. 2 where any of the three impedances can be inductive or capacitive. This topology has been selected because, depending on the values taken by the impedances during the optimization process, it allows to explore and compare the performances of the well-known and widely used series and parallel compensation networks together with those of different and still not considered solutions.

Fig.1. Equivalent circuit of a WPTS.

Fig.2. General CN with T topology and one of its realization.

3. INVERSE PROBLEM DESCRIPTION

The optimization problem is tailored to design the CNs that maximize the power P_L transferred to the load R_L and the efficiency η, defined as the ratio of the active power P_s delivered by supply generator to P_L. Both P_s and P_L are proportional the square of the amplitude V_s of the supply voltage while η, from the above definition, is independent from it; for these reasons the results of the optimization algorithm do not depend on the actual value of V_s and the following analysis has been performed considering V_s=1 V. The design variables considered in the problem are the six unknown reactances, three for each of the two CNs. The optimization

algorithm searches for the values of the design variables, and considers as given constants the other parameters of the circuit in Fig. 1, i.e. the coupling coils inductances L_t and L_r, their parasitic series resistances r_t and r_r, and the equivalent load resistance R_L.

Differently from the paper [6], here the parasitic equivalent series resistances (ESRs) of the inductive elements of the CNs are considered and modelled hypothesizing that the CN's inductors and the coupling coils were realized using the same technology and hence they have the same quality factor Q. Following to this assumption, taking as an example a CN with inductive Z_i and capacitive Z_p and Z_o, the electrical scheme given in the right side of Fig. 2 is obtained, with r_i given by:

$$r_i = \frac{\omega L_i}{Q} \tag{1}$$

where ω is the angular frequency of the supply current.

The optimization problem is based on the minimization of the two objective functions f_1 and f_2, both of them functions of the design variables. Since P_L and η have to be maximized, the objective functions are defined as:

$$\begin{aligned} f_1 &= 1 - \eta \\ f_2 &= \frac{1}{P_L} \end{aligned} \tag{2}$$

For any given set of reactances proposed by the optimization algorithm, the objective functions are computed at first solving the circuit in Fig. 1 to obtain the phasor quantities representing the current $i_s(t)$ and $i_L(t)$, then computing the values of the power P_s and P_L and finally applying the equations (2). These tasks are performed by a Matlab function written on purpose to solve step by step the circuit and to compute the objective functions. It is not viable

to reach directly their analytical expressions because they are very complicated. For example, the impedance Z_s at the power supply terminals, used to compute $i_s(t)$, is expressed in terms of the impedances of the CNs as:

$$Z_s = \frac{Z_{i,t}(j\omega L_t + r_t + Z_{p,t} + Z_{o,t} + Z_{ref}) + Z_{p,t}(j\omega L_t + r_t + Z_{o,t} + Z_{ref})}{j\omega L_t + r_t + Z_{p,t} + Z_{o,t} + Z_{ref}} \quad (3)$$

where Z_{ref} is the impedance reflected from the receiving to the transmitting stage of the WPTS, given by:

$$Z_{ref} = \omega^2 M^2 \frac{Z_{p,r} + Z_{o,r} + R_L}{(j\omega L_r + r_r + Z_{i,r})(Z_{p,r} + Z_{o,r} + R_L) + Z_{p,r}(Z_{o,r} + R_L)} \quad (4)$$

The fixed value of the parameters appearing in (3) and (4) and used to compute (2) are taken from an experimental setup [7] and reported in Table 1.

The optimization problem was solved considering two different cases. In the first case the design variables values are searched for minimizing (2) considering not-negligible ESRs (case 1); whereas in the second case (case 2), the ESRs were considered negligible.

Table 1.

Optimization algorithm

The two objective function to be minimized, f_1 and f_2, are in contrast and consequently this approach to the CNs design falls in the class of the bi-objective problems. In particular, the used

optimization algorithm belongs to the class of genetic algorithms, like e.g. NSGA-II algorithm [5]. The Matlab version of the NSGA-II algorithm was adapted by authors to solve the discussed problem; the cross over parameters were set both to 0.2 and the mutation index was set to 0.1. The design variables, that form each individual, are the 6 reactances of the CNs variable in the range [-500, +500] Ω.

4. RESULTS

The initial population was formed by N= 50 random individuals. After 250 generations the optimization algorithm converged to a set of 50 improved individuals. Then the resulting individuals were sets of impedances whose corresponding (f_1, f_2) pairs lay on a Pareto front; they are represented by circles in the upper half of Fig. 3 (case 1). In the same graph, the crosses represent the (f_1, f_2) pairs obtained applying the optimization algorithm to the same initial sets of reactances, but neglecting the effects of the ESRs (case 2). In order to give a higher meaningfulness to the representation, the (f_1, f_2) pairs have been converted into (η, P_L) pairs using (2) and then plotted in the lower half of Fig. 3 using the same code for the marks. The effects of the ESRs emerge clearly from the comparison of the Pareto fronts outlined by the marks: for a given transferred power, the maximum achievable efficiency is sensibly lower and this difference increases when high power is transferred.

Fig.3. Pairs (f_1, f_2) (up) and pairs (η, P_L) (down) relevant to the optimized CNs.

The red star in the plots in Fig. 3 represents the pairs (f_1, f_2) and (η,P_L) obtained using the series-series (SS) compensation CNs. These networks, despite their early introduction in the WPTSs field, are still object of research activity [8]; Fig. 3 shows that they are characterized by a good efficiency, but by a low transferred power.

Two peculiar behaviors can be recognized at the extremities of the Pareto fronts. In the upper half of Fig. 3, the pairs included between those marked with A and B are vertically aligned so that they are characterized by the same efficiency, which is about 0.93; the corresponding transferred power is very low, but in any way, it increases of more than 50 times moving from A to B. On the opposite extremity of the Pareto front, the pair marked with E is characterized by a comparatively very high transferred power and surprisingly lies slightly over the Pareto front obtained neglecting the ESRs. In the middle of the Pareto front, the pairs included between those marked with C and D exhibit a smooth transition from CNs that assure a high efficiency and somewhat low power to CNs characterized by acceptable efficiency and comparatively high power. The efficiency and the transferred power relevant to the pairs A-E and to the SS CNs are listed in the second and third columns of Table 2; the corresponding reactances are reported in the rightmost columns of the table.

Table 2.

Evaluation of the results

The objective functions have been computed under the hypothesis of sinusoidal currents in the CNs elements and in the coupling coils. This hypothesis is verified if both the CNs or, at least, CN_t, act as a filter for the supply current. This condition can be easily verified by the analysis of the Bode diagrams relevant to the circuit of Fig. 1 endowed with the CNs belonging to the Pareto front. In particular, the magnitude Bode diagram of the supply current $i_s(t)$, of the coils currents $i_t(t)$ and $i_r(t)$, and of the load current $i_L(t)$ are considered.

The magnitude Bode diagrams relevant to pair A are plotted in Fig. 4 using the blue solid line for I_s, the dashed green line for I_t, the black solid line for I_r and the red dashed line for I_L. Clearly, it appears that I_s increases with the angular frequency so that a square wave supply

voltage will originate a high frequency content in $i_s(t)$. The Bode diagrams of the other currents exhibits a filtering effect, but it is not strong enough to force the currents to be sinusoidal: the amplitude of the first and the third harmonic of $i_t(t)$ are nearly equal while the attenuation of the harmonics of $i_r(t)$ and $i_L(t)$ is only a little more effective. The Bode diagram relevant to pair B has a similar behavior and is not reported here.

Fig.4. Amplitude Bode diagram relevant to point A.

The Bode diagrams related to pair C are reported in Fig. 5. They show a good filtering action of the high frequency harmonics of $i_s(t)$ and an even stronger attenuation of the harmonics of the other currents. On the other hand, the peaks of resonance do not correspond to the supply angular frequency and hence the latter one should be carefully controlled to protect the system against undue over-currents caused by a supply frequency higher than the nominal one.

Fig.5. Amplitude Bode diagram relevant to point C.

The pair E originates the Bode diagrams reported in Fig. 6; the pair D has similar diagrams not reported here. In this case, there is a sensible filtering effect for all the currents and there is a peak of resonance at the supply frequency. These conditions force the WPTS to operate with currents nearly sinusoidal and make reliable the values of η and P_L computed using the equivalent circuit of Fig. 1.

Fig.6. Amplitude Bode diagram relevant to point E.

These conclusions have been verified in the Simulink environment, simulating the behavior of the WPTS supplied with a square wave voltage having a first harmonic amplitude of 1 V. As an example, the waveforms of the supply voltage and current relevant to pairs A and E are plotted in the upper half of Figs. 7 and 8, respectively. In the lower halves of the figures the currents $i_t(t)$, $i_r(t)$ and $i_L(t)$ are drawn. As expected, the graphs obtained with pair A are highly distorted, with $i_s(t)$ oscillating at a so high frequency that in the given time scale it is not possible to recognize its actual waveform; similar behavior is obtained also considering pair B. The current waveforms obtained from pairs C, D, and E are nearly sinusoidal and are characterized by a decreasing phase difference between $v_s(t)$ and $i_s(t)$ and by having $i_r(t)$ and $i_L(t)$ nearly in phase.

From this analysis it results that each pair obtained from the optimization algorithm has to be checked before implementation since, as discussed before, it could result not effective and/or not robust against system uncertainty. For example, implementation of pair A could cause a fault of the supply inverter due to the uncontrolled high frequency components of the current waveform.

Fig.7. Voltage and currents in the WPTS with CNs corresponding to pair A.

Fig.8. Voltage and currents in the WPTS with CNs corresponding to pair E.

Powers P_s and P_L achieved for the five considered T-CNs and for the SS CNs have been worked out by averaging over one supply period the product of the samples of voltage and current at the inverter output and at the equivalent load input. From them, the efficiency derives immediately as power ratio. The obtained values are listed in the fourth and fifth columns of Table 2. With the exception of those relevant to pair A, they match perfectly with the results

coming from the circuital equations used to compute the objective functions thus validating the proposed design approach.

5. CONCLUSIONS

The paper presented the application of an optimization algorithm to the design of the compensation networks of a WPTS. This approach gave interesting results and made available a number of different sizing solutions of complex networks in a very short time. Most of the obtained solutions outperform the widely-used SS compensation; but it has been shown that an accurate post processing of the obtained result is mandatory in order to discriminate the solutions that could actually be implemented from those that in a real system would not give acceptable performance because of uncontrolled high frequency current oscillation.

REFERENCES

[1] Covic, C.A. and Boys, J.T. (2013) Inductive power transfer, Proceedings of the IEEE, Vol. 101, no. 6, pp. 1276–1289.

[2] Li, R. (2017) Design of dual-band coil for wireless power transfer system via magnetic resonant coupling, International Journal of Applied Electromagnetics and Mechanics, Vol. 53, no. 3, pp. 511-521.

[3] Feng, H., Cai, T., Duan, S., Zhang, X., Hu, H., and Niu, J. (2018) A dual-side-detuned series–series compensated resonant converter for wide charging region in a wireless power transfer system, IEEE Transactions on Industrial Electronics, Vol. 65, no. 3, pp. 2177–2188.

[4] L. Xiang, Y.Sung, X. Dai, C. Tang, and C. Hu. (2017) Evaluation of magnetic coupler for stationary EVs' wireless charging, International Journal of Applied Electromagnetics and Mechanics, Vol. 53, no. 1, pp. 167-179.

[5] Deb, K., Pratap, A., Agarwal, S., and Meyarivan, T. (2002) A fast and elitist multiobjective genetic algorithm: NSGA-II IEEE Transactions on Evolutionary Computation, Vol. 6, no. 2, pp. 182–197.

[6] Bertoluzzo, M, Forato, M, and Sieni, E. (2018) Optimization of the Compensation Networks for WPT Systems, Proceedings of IECON.

[7] Buja, G. Bertoluzzo, M., and Mude, K. N (2015) Design and Experimentation of WPT charger for electric city car IEEE Transactions on Industrial Electronics, Vol. 62, no. 12, pp. 7436–7447.

[8] M. Forato, M., Bertoluzzo, M. (2018) Modified series-series compensation topology for WPT systems, " Proceedings of IEEE PELS.

TABLES

Table 1: fixed values of the WPTS parameters.

Parameter	**Symbol**	**Value**
Transmitting coil inductance	L_t	120 μH
Receiving coil inductance	L_r	120 μH
Coils ESR	r_t, r_r	0.5 Ω
Coil quality factor	Q	128
Mutual inductance	M	30 μH
Supply angular frequency	ω	2π·85000 rad/s
Supply voltage	V_s	1 V

Table 2: Efficiency and transferred power for different CNs

CNs	**η**	**P_L [mW]**	**η_{sim}**	**$P_{L,sim}$ [mW]**	**$X_{i,t}$ [Ω]**	**$X_{p,t}$ [Ω]**	**$X_{o,t}$ [Ω]**	**$X_{i,r}$ [Ω]**	**$X_{p,r}$ [Ω]**	**$X_{o,r}$ [Ω]**
A	0.93	0.16	0.35	0.16	-193.57	-228.65	-87.34	-43.59	41.16	-14.90
B	0.93	8.12	0.93	8.11	-10.32	-436.26	-82.32	-45.00	39.86	-15.22
C	0.90	91	0.90	91	8.07	-11.07	-75.28	-24.00	497.20	-40.23
D	0.80	1203	0.80	1204	3.97	-4.58	-74.19	-25.32	496.04	-29.26
E	0.64	2278	0.63	2720	3.69	-4.44	-74.55	-23.70	494.42	-18.25
SS	0.91	11	0.91	11	-32.04	n.a.	-32.04	-32.04a.	n.a.	-32.04

FIGURE CAPTIONS

Fig.1. Equivalent circuit of a WPTS.

Fig.2. General CN with T topology and one of its realization.

Fig.3. Pairs (f_1, f_2) (up) and pairs (η, P_L) (down) relevant to the optimized CNs.

Fig.4. Amplitude Bode diagram relevant to point A.

Fig.5. Amplitude Bode diagram relevant to point C.

Fig.6. Amplitude Bode diagram relevant to point E.

Fig.7. Voltage and currents in the WPTS with CNs corresponding to pair A.

Fig.8. Voltage and currents in the WPTS with CNs corresponding to pair E.

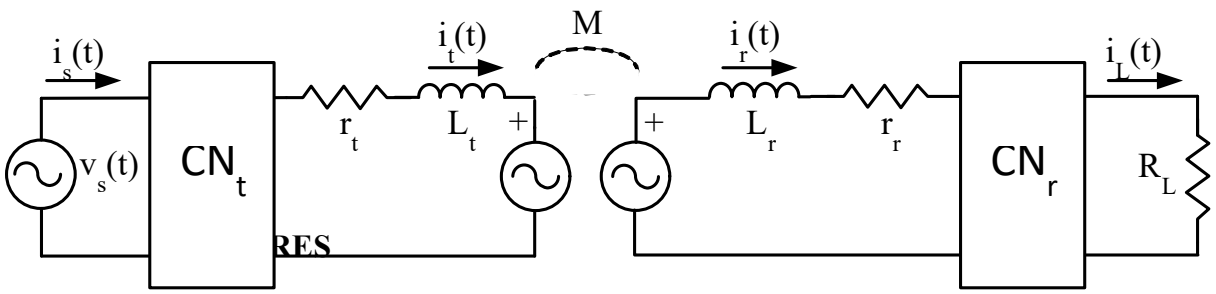

Fig.1. Equivalent circuit of a WPTS.

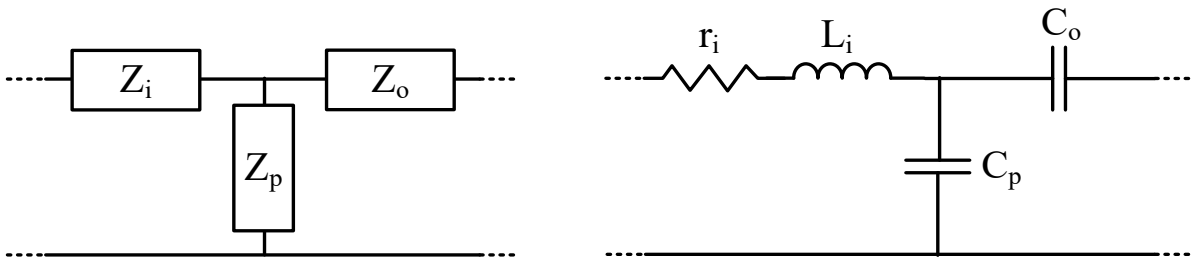

Fig.2. General CN with T topology and one of its realization.

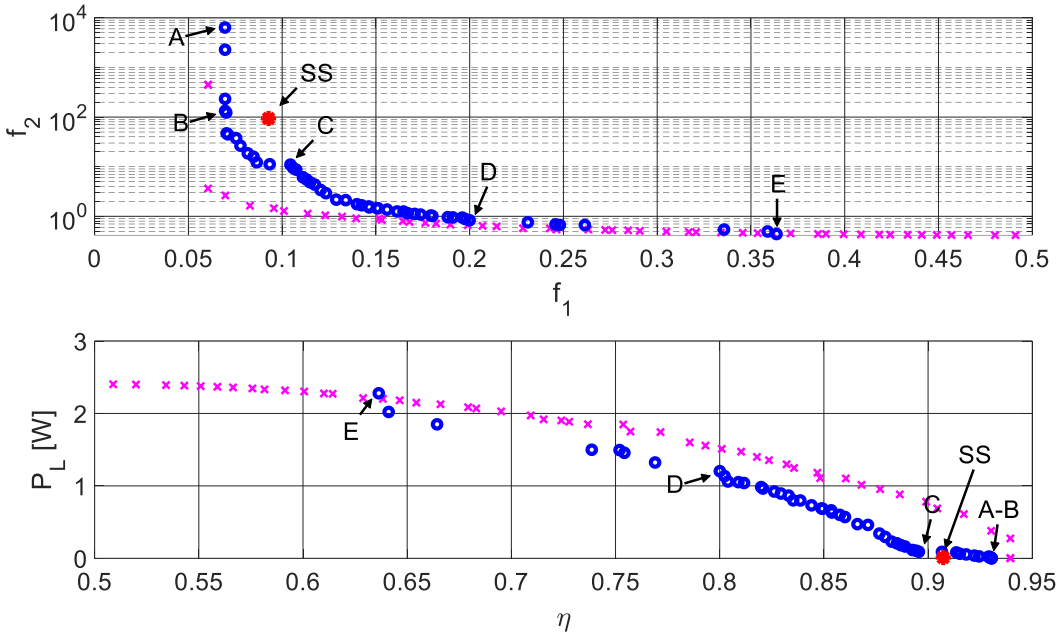

Fig.3. Pairs (f_1, f_2) (up) and pairs (η, P_L) (down) relevant to the optimized CNs

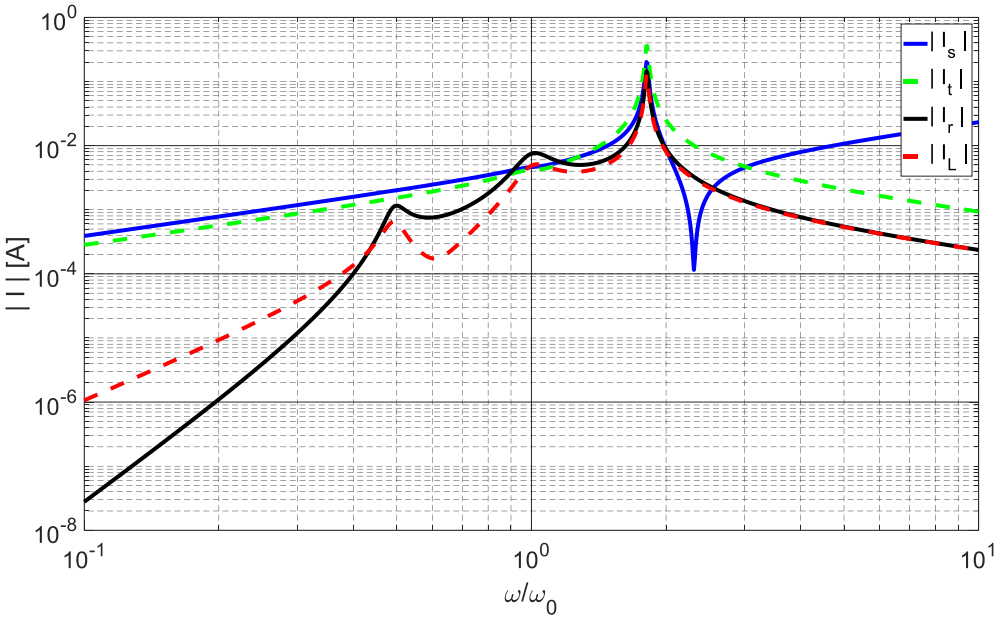

Fig.4. Amplitude Bode diagram relevant to point A.

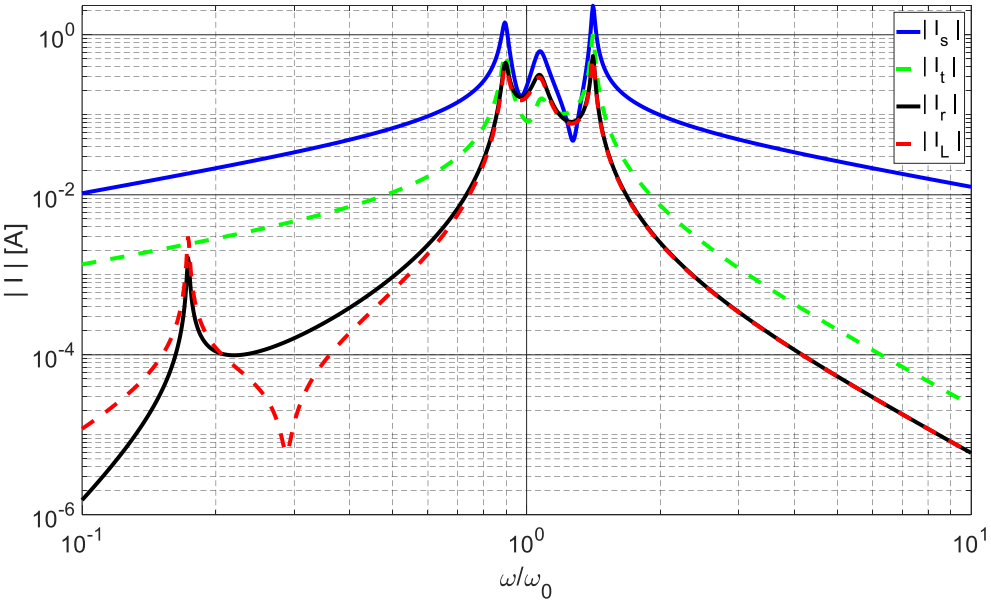

Fig.5. Amplitude Bode diagram relevant to point C.

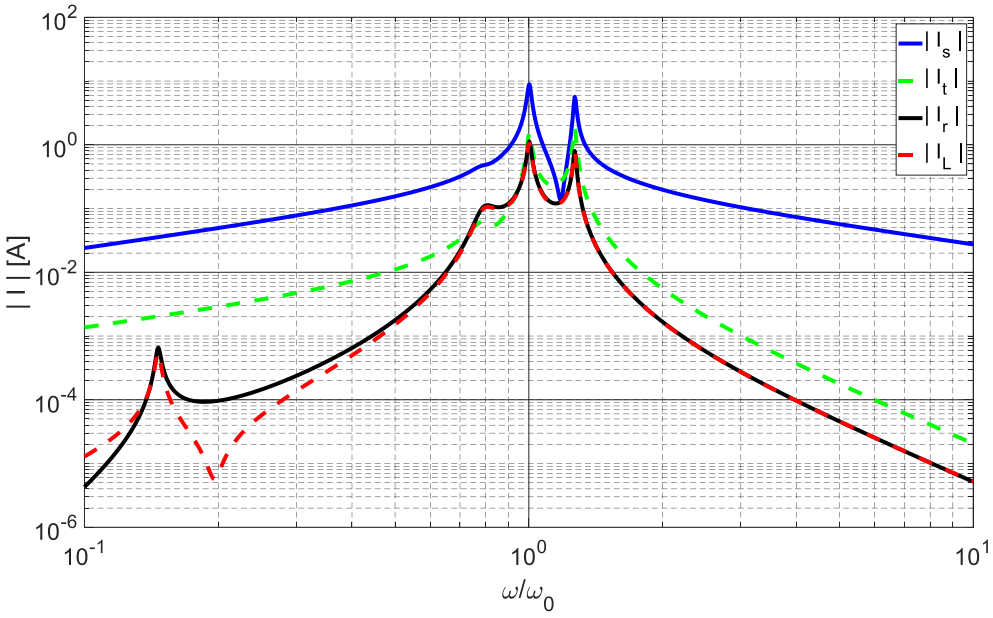

Fig.6. Amplitude Bode diagram relevant to point E.

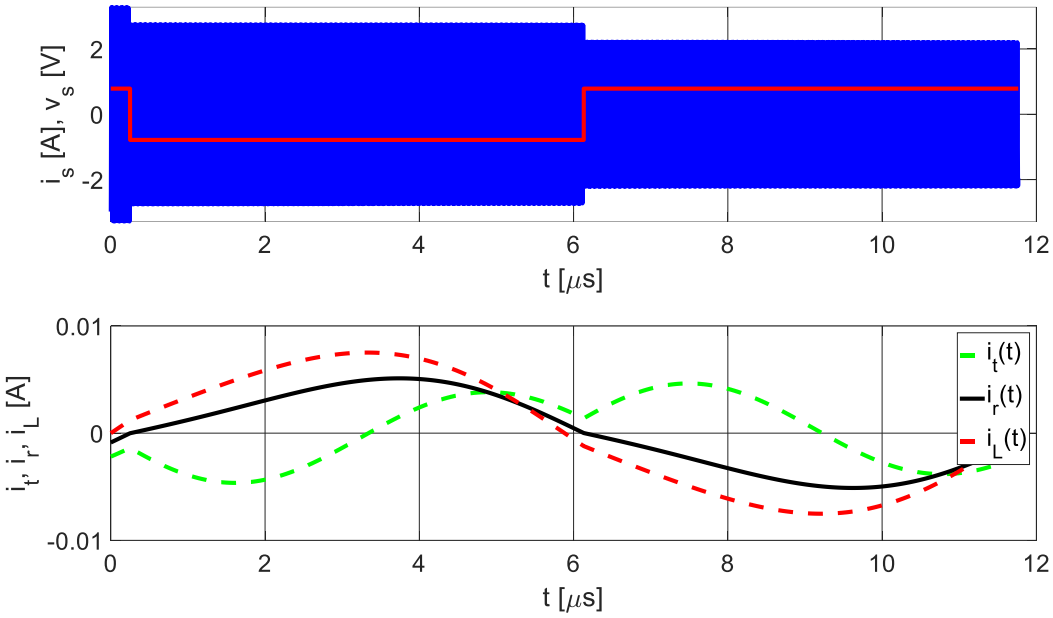

Fig.7. Voltage and currents in the WPTS with CNs corresponding to pair A.

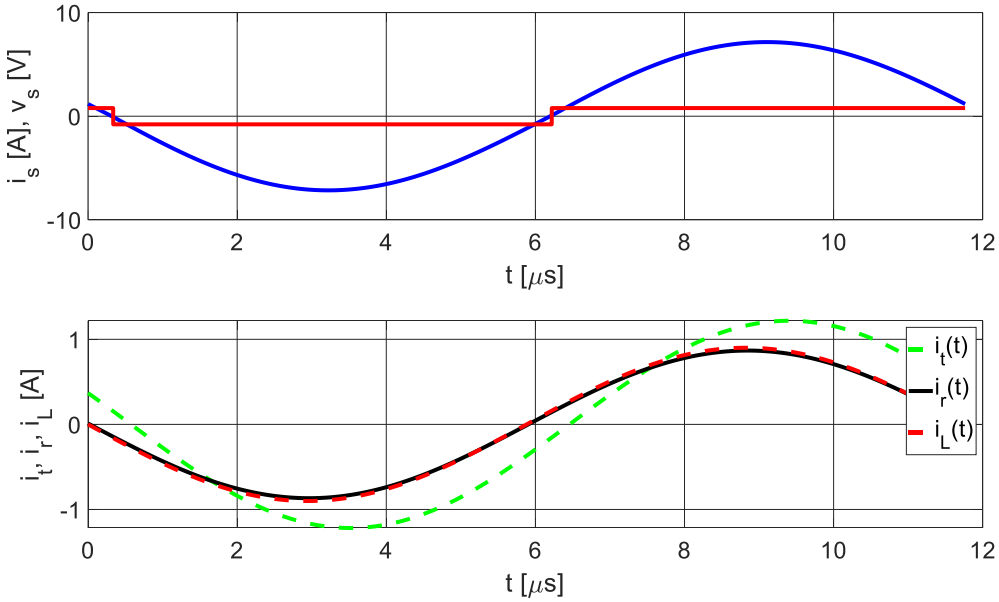

Fig.8. Voltage and currents in the WPTS with CNs corresponding to pair E.